Investigation of a Canonical All-Movable Control Surface in Thickened Boundary Layers

Chris L. Ellis[1,2], David B. Clarke[1], Daniel Butler[1] and Paul Brandner[2]

[1]Hydroacoustics Group, Maritime Division, Defence Science and Technology Group, Fishermans Bend, Victoria, 3207, Australia.
[2] Cavitation Research Laboratory, Australian Maritime College, University of Tasmania, Launceston, Tasmania, 7250, Australia.

Abstract

Submarine aft control surfaces are low aspect ratio appendages that operate, under normal conditions, with a significant portion of their span submerged in the hull boundary layer. These aft control surfaces have a significant gap between the root and hull when placed at incidence. The loads and stall behaviour of these control surfaces are of interest as they directly influence a submarines ability to maneuver, maintain stability and impact the spatial and temporal uniformity of the flow into the propeller. The hull boundary layer and the root-hull gap have a significant influence on the control surface performance.

The cavitation tunnel at the Australian Maritime College (AMC) Cavitation Research Laboratory (CRL) can produce a range of thickened and thinned boundary layers on its ceiling. This capability was used to create a boundary layer with similar momentum deficit to that which occurs at the aft of a submarine. This allows us to obtain force measurements more representative of the conditions on a real submarine for a submarine aft control surface. The loads and stall behaviour of a canonical all-movable control surface were investigated for a range of boundary layer thicknesses and root gap sizes. An increased root gap was observed to increase stall angles and reduce the lift curve slope at low angles of incidence. The thickened boundary layers were observed to have a significant influence on the load measurements during stall, with reduced hysteresis, increased maximum lift and increased stall angle. A momentum based estimate was effective in accounting for the influence of the thickened boundary layer on the measured loads.

Introduction

There is an extensive range of control surface geometries currently in use on operating submarines. This demonstrates that there is not a widely accepted standard design. While an all-movable control surface is likely to provide the greatest lift for a given planform area, it may prove to be less rigid than a flapped control surface composed of a fixed stabiliser and moving flap. The shape of the control surface tip and size of the root gap also play a role in the hydrodynamic, signature and cavitation performance of the control surface. The stabiliser may also provide locations to mount ancillary equipment that would not be practical on an all-movable control surface.

The aft control surface on a submarine operates in a complex flow field with spatial and temporal variations that increase as the submarine changes direction. Even in straight ahead conditions the aft control surfaces operate in a relatively thick boundary layer that continues to thicken notably as it moves downstream. This creates an environment with reduced momentum and increased turbulent intensities close to the hull. The boundary layer thickening capability of the cavitation tunnel at the AMC CRL was used to emulate this boundary layer condition.

Early work by Fehlner[3] demonstrated that the combination of maximum lift coefficient, C_{Lmax}, and drag coefficient, C_D, may be used to optimise the size and planform of the control surface, while the lift against angle of incidence coefficient, $C_{L\alpha}$, is important when considering the stability of a vessel. Fehlner also showed that the lift coefficient, C_L, generated by an all-movable control surface, for a given planform area and angle of incidence, is greater than that of a flapped control surface at the same conditions.

Molland[6] also conducted an extensive study into the characteristics of rudder design for small craft. Many of these design characteristics are applicable to larger and/or submersible craft. Molland observed, with respect to all-movable control surfaces, that the lift on the control surface comprises of two components, one arising from the flow in the longitudinal plane and the other from the cross-flow associated with the small aspect ratio typical of marine applications. Molland also found that an increase in the root gap causes the lift produced by the control surface to decrease, a root gap of 0.011c (where c is the chord length) caused lift to decrease by approximately 5%. The influence of the root gap was studied by considering it as a reduction of the aspect ratio.

Sarraf et al.[7] investigated the influence of section thickness on symmetric NACA sections. The study was performed using a NACA0015, NACA0025 and NACA0035 section that spanned the test section for a Reynolds number, Re, based on chord length, of 0.5×10^6. Flow field measurements were carried out using laser Doppler velocimetry (LDV) and particle image velocimetry (PIV); while loads were measured using a force balance. They reported that the linear lift behaviour of the NACA0015 profile was limited to angles of incidence lower than 7°, with stall, and a corresponding jump in C_D, occurring at an angle of incidence of 21°. Once stall occurred, reducing the angle of incidence did not result in flow reattachment until an angle of incidence of 15°. The upper branch of the load hysteresis loop from 15° to 20° was distinguished by partial flow separation where the detachment point progressively moves upstream from the trailing edge to the leading edge as the angle of incidence is increased. The lower branch of the hysteresis loop from 21° to 16° was distinguished by massive flow separation.

This paper examines the loads and stall behaviour of a canonical all-movable submarine aft control surface in thickened and thinned boundary layers, with various root gaps and over a range of Reynolds numbers.

Experimental Method, Model and Facility

Model

A hydrofoil with a NACA0015 section, 140 mm root chord, taper ratio of 0.8, no trailing edge sweep, semi-span equal to root chord

and an aspect ratio of 2.22 was chosen to represent a canonical submarine all-movable control surface (Figure 1). The coordinate system is aligned with the x-axis being in the flow direction and positive from leading edge to trailing edge, and the z-axis being in the spanwise direction, with positive from root to tip away from the test section ceiling.
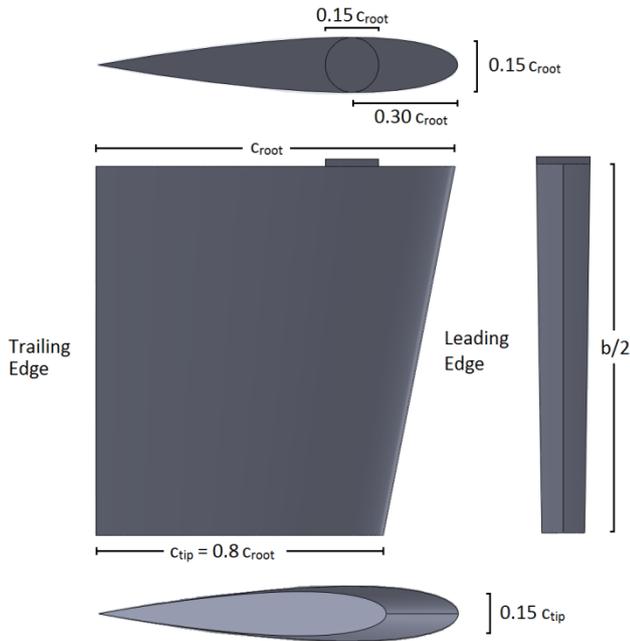
Figure 1. Canonical control surface design: NACA0015 section, taper ratio 0.8, no trailing edge sweep, and semispan equal to root chord.

By including a spacer of different thicknesses in the mounting flange, the root gap could be easily modified. The root gaps tested for the control surface were $0.0036\,c_{root}$, $0.025\,c_{root}$ and $0.046\,c_{root}$ (or 0.5 mm, 3.5 mm and 6.5 mm, respectively). The control surface was manufactured from type 316 stainless steel. Metrology performed on the control surface reported that for the vast majority of the control surface a tolerance of better than 0.05 mm was achieved.

The control surface model flow was tripped using commercially available trip strips, with a height of 63.5 μm at a location of $x/c = 0.15$. The trip strip was comprised of circular elements of 1.27 mm diameter spaced 2.54 mm between centres.

The Reynolds number based on the control surface root chord, Re_{root}, is used throughout this paper as the reference Reynolds number.

Cavitation Tunnel

The AMC CRL cavitation tunnel is a closed circuit variable pressure water tunnel[1] with a test section of 600 mm x 600 mm cross sectional area. The bottom surface of the test section has a 0.44° slope to compensate for boundary layer growth giving it an exit height of 0.620 mm. A Computer Aided Design (CAD) image of the physical layout of the facility is shown in Figure 2. The tunnel can operate at pressures from 4 kPa to 400 kPa absolute and flow speeds between 2 m/s and 12 m/s. This allows the Re, based on tunnel width, of $O(10^6)$ to be achieved. The tunnel is filled with demineralised water.

The cavitation tunnel has a boundary layer thickening and suction capability on the ceiling of the test section. An increased boundary layer thickness is more representative of the conditions that exist at the aft control surfaces of a submarine. The ceiling boundary layer, depending on streamwise location, may be varied between approximately 10 mm and 100 mm. The thickness of the

ceiling boundary layer is controlled through the injection ratio,

$$C_{p\_inj} = \frac{2\Delta P_{plen}}{\rho U_\infty^2},$$

where ΔP_{plen} is the nominal static pressure differential between the plenum and a location opposite the injection thickening plate, U_∞ is the free-stream velocity in the test section and ρ is the fluid density (Figure 3). The injection and suction was performed through a perforated plate centred 178 mm upstream of the start of the test section. A schematic of the plenum and testing locations are shown in Figure 3.
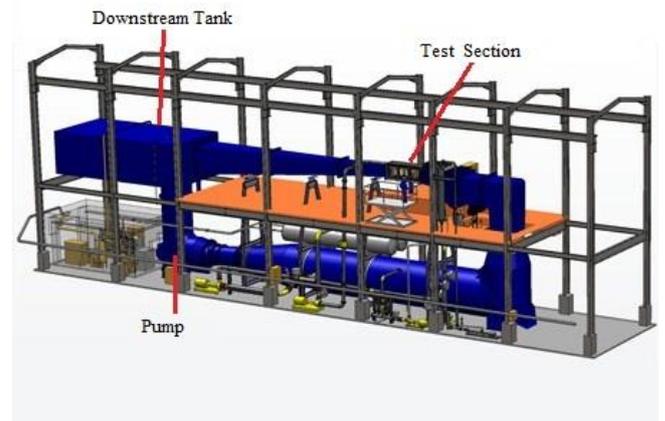
Figure 2. CAD image of the AMC cavitation tunnel[1].

The boundary layer profiles generated by the thickening and suction capability at $Re_{root} = 1.0 \times 10^6$ for a range of injection ratios are shown in Figure 4. Also shown is the velocity profile in the vicinity of the aft control surfaces (for the Joubert hullform) where $2z/b$ is the non-dimensional distance from the test section ceiling (or hull). The Joubert hullform is a generic submarine shape designed by Joubert[4][5] and developed by DST Group to provide a 'generic' submarine hullform typical of a diesel submarine (Figure 5).
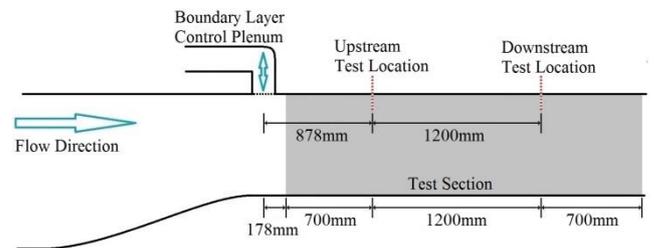
Figure 3. Schematic showing location of boundary layer control plenum and test positions in the AMC cavitation tunnel.

Given the significantly different conditions that exist in the test section to that at the aft of the submarine, it would be a considerable undertaking to create a boundary layer on the test section ceiling with a velocity profile that closely matches the one that exists at the aft of the submarine. The approach taken was to generate a boundary layer on the test section ceiling that would create a similar loading condition on the control surface. The boundary layer produced with a $C_{P,inj}$ of 0.440 was determined to create a representative loading condition for the control surfaces on the Joubert hullform[4][5].
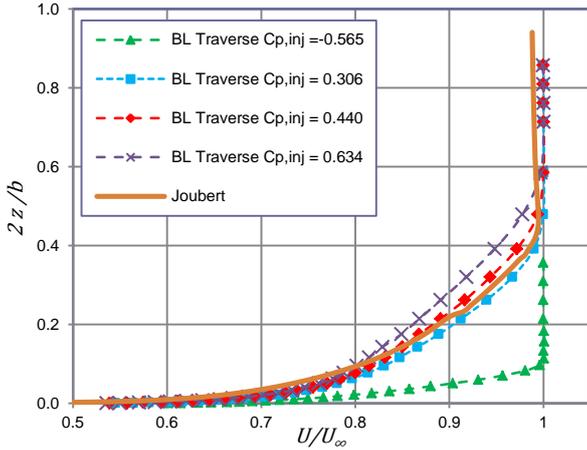
Figure 4. Measured boundary layer profiles at $Re_{root} = 1.0 \times 10^6$ and nominal boundary layers profiles in vicinity of aft control surface for the Joubert hullform[4][5].
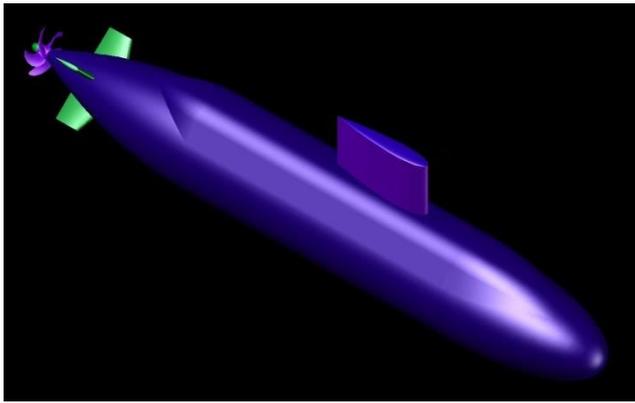
Figure 5. Fully appended Joubert 'generic' diesel submarine hullform.

Force Balance

A six component force balance used for these measurements comprised of a rotating spindle supported in the centre of a heavy stainless steel superstructure, which is flooded to equalise the pressure on the measurement disk[2]. Its rotation is tracked by an absolute optical encoder. The measurement disk, where the test item is mounted, is connected to the spindle by six beam load cells and flexures. These are arranged in two triangular configurations to resolve 3 orthogonal forces and their corresponding moments. The balance is calibrated using slung masses, accurately aligned in the primary forcing directions. By applying a series of known loads in specific directions and measuring the load cells responses an inverse calibration matrix is formed. The balances response to the forcing, over the load ranges used, has been demonstrated to be linear[2].

Results

Influence of ceiling-root gap

The influence of changing the ceiling root gap is most pronounced in the case with a thinned boundary layer ($C_{p\_inj} = -0.565$). Figure 6 shows that increasing the ceiling root gap:

- increased stall angle;
- increased C_{Lmax} for the highest Re_{root} of 1.25×10^6;
- reduced $C_{L\alpha}$ at low angles of incidence; and
- increased C_D.

For the cases with the thickened boundary layer, the trend of increasing C_{Lmax} with increasing gap size no longer exists. That being said, C_{Lmax} is larger by approximately 10% (Figure 7) and $C_{L\alpha}$ is less than observed with the thinned boundary layer.
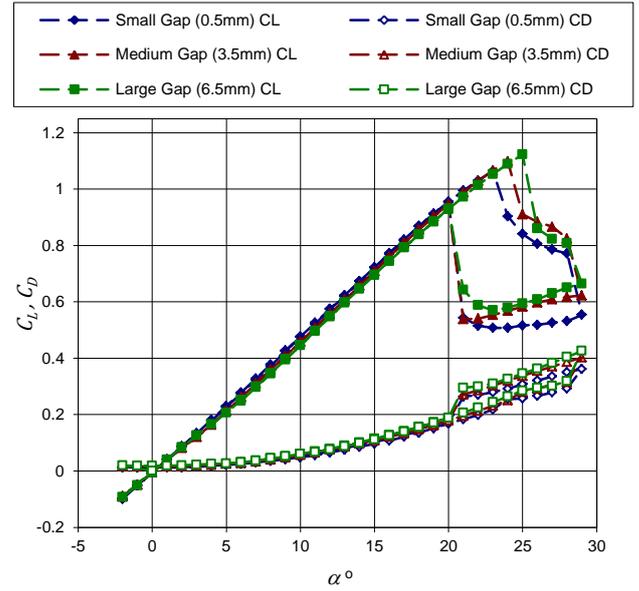
Figure 6. Lift and drag coefficients for the control surface with gap size for a Re_{root} of 1.25×10⁶ with an injection ratio of $C_{p\_inj} = -0.565$. The filled symbols represent the lift coefficient, C_L and the hollow symbols show the drag coefficient, C_D.
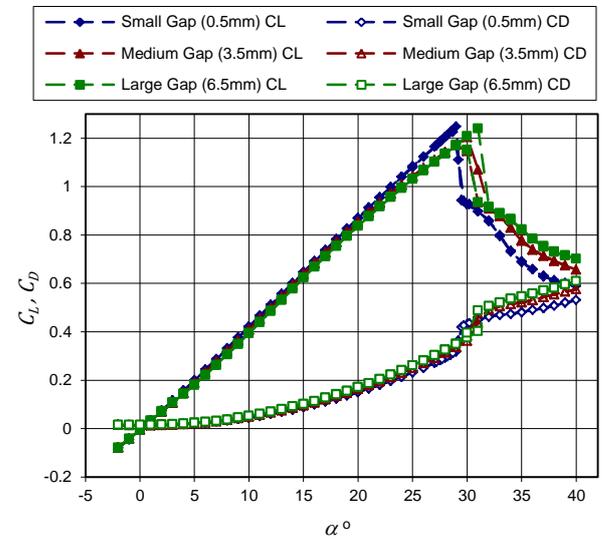
Figure 7. Lift and drag coefficients for the control surface with gap size for a Re_{root} of 1.25×10⁶ with an injection ratio of $C_{p\_inj} = 0.440$. The filled symbols represent the lift coefficient, C_L and the hollow symbols show the drag coefficient, C_D.

Influence of boundary layer thickness

The influence of increasing the boundary layer thickness was examined using four boundary layer thicknesses. For the smallest root gap at $Re_{root} = 1.25 \times 10^6$, an increased boundary layer thickness resulted in:

- increased stall angle;
- slightly reduced $C_{L\alpha}$;
- increased C_{Lmax};
- slightly decreased C_D; and
- reduced stall hysteresis,

as observed in Figure 8.
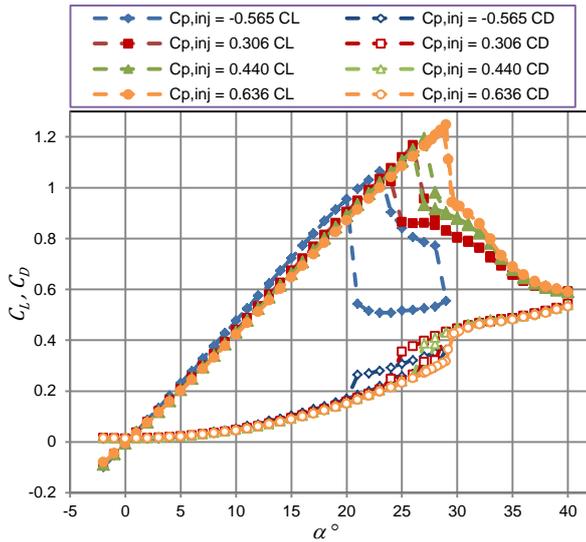
Figure 8. Lift and drag coefficients for the control surface with boundary layer thickness for a Re_{root} of 1.25×10^6 with a small gap (0.5 mm). The filled symbols represent the lift coefficient, C_L and the hollow symbols show the drag coefficient, C_D.

The increase in stall angle is caused by the increased turbulence in the thickened ceiling boundary layer, which transports energy into the boundary layer on the control surface, preventing separation. The thickened boundary layer results in a slight reduction in the average flow velocity across the control surface, reducing $C_{L\alpha}$. Despite the small reduction in $C_{L\alpha}$, an increase in C_{Lmax} is still observed, due to the significant increase in stall angle.

The change in post stall behaviour is notable due to the different boundary layers. The large hysteresis loop that exists for the load curves with the thinned boundary layer is reduced to nothing by the increased turbulence in the thickest boundary layer. This hysteresis is associated with the stalled control surface creating a stable flow that requires a reduction in the angle of incidence below the inception stall angle. The turbulence associated with the thickened boundary layer disrupts this stable flow thus reducing the hysteresis loop.

Influence of Reynolds number

Figure 9 shows a comparison of lift and drag coefficient against angle of incidence for a range of Reynolds numbers.

The primary influence of Reynolds number on the behaviour of the control surface is observed in the hysteresis behaviour. The stall is more gradual at greater Reynolds numbers, indicating partial flow separation is maintained at greater angles of incidence. The hysteresis loop also closes at slightly lesser angles of incidence for lower Reynolds numbers. $C_{L\alpha}$, C_D and C_{Lmax} display very little dependency on Reynolds number.

Conclusions

A canonical all-movable aft control surface representative of those used on submarines has been designed and studied at the AMC cavitation tunnel. The influence of boundary layer thickness, root gap and Reynolds number on the loads generated by this control surface has been investigated.

A thickened boundary layer, representative of the flow conditions present at the rear of a submarine, was generated at the AMC cavitation tunnel. The thickened boundary layer was observed to increase stall angle and C_{Lmax} and significantly reduce the stall hysteresis. The reduction, and almost elimination, of the stall hysteresis loop results in simpler load curves.
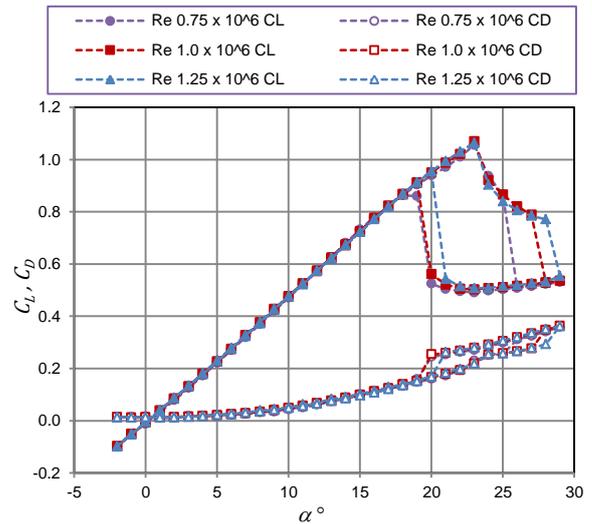
Figure 9. Lift and drag coefficients for the control surface with a gap size of 0.5mm and $C_{p\_inj} = -0.565$ for a Re_{root} between 0.5×10^6 and 1.25×10^6. The filled symbols represent the lift coefficient, C_L, and the hollow symbols show the drag coefficient, C_D.

Increased root gaps were observed to increase stall angle, increase C_D and reduce $C_{L\alpha}$ at low angles of incidence. For the thinned boundary layer, C_{Lmax} is observed to increase with an increased root gap, though this trend is not observed with the thickened boundary layer. Due, at least in part, to the use of trip strips, only the stall behaviour demonstrated a dependency on Reynolds number, with the higher Reynolds numbers showing more gradual stall and the hysteresis loop closing at slightly higher angles of incidence.

References

[1] Brandner, P.A., Lecoffre, Y. and Walker, G.J., 2007, *Design considerations in the Development of a Modern Cavitation Tunnel,* 16th Australasian Fluid Mechanics Conference, Gold Coast, Queensland, pp. 630-637.

[2] Butler, D., Smith, S.M, Brandner, P.A., Clarke, D.B., Pearce, B.W., 2018, *Static calibration and dynamic behaviour of a six-component force balance for variable pressure water facilities,* J. Exp. Mech., Currently under review.

[3] Fehlner, L.F., 1951, *The Design of Control Surfaces for Hydrodynamic Applications,* David Taylor Model Basin Report C-358, URI: http://hdl.handle.net/1721.3/51150

[4] Joubert, P.N. Some Aspects of Submarine Design Part 1. Hydrodynamics, *DSTO-TR-1622,* Platform Sciences Lab, Defence Science and Technology Organisation, Victoria, Australia, 2004.

[5] Joubert, P.N. Some Aspects of Submarine Design Part 2. Shape of a Submarine 2026, *DSTO-TR-1920,* Platform Sciences Lab, Defence Science and Technology Organisation, Victoria, Australia, 2006

[6] Molland, A.F., 1987, *Rudder design data for small craft,* Southampton, UK, University of Southampton, Ship Science Report No. 1/78, p66

[7] Sarraf, C., Djeridib, H., and Billard, J.Y., 2010, *Thickness effect of NACA foils on hydrodynamic global parameters, boundary layer states and stall establishment,* Journal of Fluids and Structures, vol 26, issue 4, pp 55